

ResAct: Reinforcing Long-term Engagement in Sequential Recommendation with Residual Actor

Wanqi Xue^{1*}, Qingpeng Cai², Ruohan Zhan^{3†}, Dong Zheng², Peng Jiang², Bo An¹

¹Nanyang Technological University

²Kuaishou Technology

³Stanford University

Abstract

Long-term engagement is preferred over immediate engagement in sequential recommendation as it directly affects product operational metrics such as daily active users (DAUs) and dwell time. Meanwhile, reinforcement learning (RL) is widely regarded as a promising framework for optimizing long-term engagement in sequential recommendation. However, due to expensive online interactions, it is very difficult for RL algorithms to perform state-action value estimation, exploration and feature extraction when optimizing long-term engagement. In this paper, we propose ResAct which seeks a policy that is close to, but better than, the online-serving policy. In this way, we can collect sufficient data near the learned policy so that state-action values can be properly estimated, and there is no need to perform online exploration. Directly optimizing this policy is difficult due to the huge policy space. ResAct instead solves it by first reconstructing the online behaviors and then improving it. Our main contributions are fourfold. First, we design a generative model which reconstructs behaviors of the online-serving policy by sampling multiple action estimators. Second, we design an effective learning paradigm to train the residual actor which can output the residual for action improvement. Third, we facilitate the extraction of features with two information-theoretical regularizers to confirm the expressiveness and conciseness of features. Fourth, we conduct extensive experiments on a real-world dataset consisting of millions of sessions, and our method significantly outperforms the state-of-the-art baselines in various of long-term engagement optimization tasks.

1 Introduction

In recent years, sequential recommendation has achieved remarkable success in various fields such as news recommendation [35, 40, 5], digital entertainment [6, 14, 22], E-commerce [4, 31] and social media [38, 23]. Real-life products, such as Tiktok³, have influenced the daily lives of billions of people with the support of sequential recommender systems. Different from traditional recommender systems which assume that the number of recommended items is fixed, a sequential recommender system keeps recommending items to a user until the user quits the current service/session [34, 13]. In sequential recommendation, as depicted in Figure 1, users have the option to browse endless items in one session and can restart a new session after they quit the old one [39]. To this end, an ideal sequential recommender system would be expected to achieve i) low return time between sessions, i.e., high frequency of user visits; and ii) large session length so that more items can be

*Correspondence to wanqi001@e.ntu.edu.sg

†Work done at Kuaishou Technology

³<https://www.tiktok.com/>

browsed in each session⁴. We denote these two characteristics, i.e., return time and session length, as long-term engagement, in contrast to immediate engagement which is conventionally measured by click-through rates [13]. Long-term engagement is preferred over immediate engagement in sequential recommender systems because it directly affects product operational metrics such as daily active users (DAUs) and dwell time.

Despite great importance, unfortunately, how to effectively improve long-term engagement in sequential recommendation remains largely uninvestigated. Existing works on sequential recommendation have typically focused on estimating the probability of immediate engagement with various neural network architectures [13, 31, 28]. However, they neglect to explicitly improve user stickiness such as increasing the frequency of visits or extending the average session length. There have been some recent efforts to optimize long-term engagement in sequential recommendation. How-

ever, they are usually based on strong assumptions such as recommendation diversity will increase long-term engagement [32, 41]. In fact, the relationship between recommendation diversity and long-term engagement is largely empirical, and how to measure diversity properly is also unclear [39].

Recently, reinforcement learning has achieved impressive advances in various sequential decision-making tasks, such as games [27, 24], autonomous driving [17] and robotics [19]. Reinforcement learning in general focuses on learning policies which maximize cumulative reward from a long-term perspective [29]. To this end, it offers us a promising framework to optimize long-term engagement in sequential recommendation [2]. We can formulate the recommender system as an agent, with users as the environment, and assign rewards to the recommender system based on users’ response, for example, the return time between two sessions. However, back to reality, there are significant challenges. First, the evolvement of user stickiness lasts for a long period, usually days or months, which makes the evaluation of state-action value difficult. Second, probing for rewards in previously unexplored areas, i.e., exploration, requires live experiments and may hurt user experience. Third, rewards of long-term engagement only occur at the beginning or end of a session and are therefore sparse compared to immediate user responses. As a result, representations of states may not contain sufficient information about long-term engagement.

To mitigate the aforementioned challenges, we propose to learn a recommendation policy that is close to, but better than, the online-serving policy. In this way, i) we can collect sufficient data near the learned policy so that state-action values can be properly estimated; and ii) there is no need to perform online exploration. However, directly learning such a policy is quite difficult since we need to perform optimization in the entire policy space. Instead, our method, ResAct, achieves it by first reconstructing the online behaviors of previous recommendation models, and then improving upon the predictions by imposing a residual. The original optimization problem is decomposed into two sub-tasks which are easier to solve. Furthermore, to better representations, two information-theoretical regularizers are designed to confirm the expressiveness and conciseness of features. We conduct experiments on a real-world dataset consisting of millions of sessions. The results show that ResAct significantly outperforms the state-of-the-art baselines in various long-term engagement optimization tasks.

2 Problem Statement

In sequential recommendation, users interact with the recommender system on a session basis. A session starts when a user opens the App and ends when he/she leaves. As in Figure 1, when a user starts a session, the recommendation agent begins to feed items to the user, one for each recommendation request, until the session ends. For each request, the user can choose to consume the recommended item or quit the current session. A user may start a new session after he/she exits the old one, and can consume an arbitrary number of items within a session. An ideal recommender system with a goal for long-term engagement would be expected to minimize the average return time between sessions while maximizing the average number of items consumed in a session. Formally,

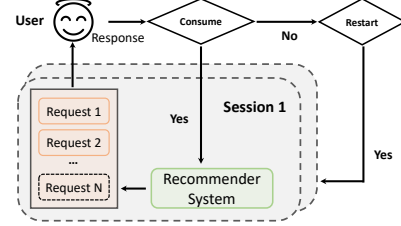


Figure 1: Sequential recommendation.

⁴Each recommendation is counted as one request, and session length is the number of requests contained in a session.

we describe the sequential recommendation problem as a Markov Decision Process (MDP) which is defined by a tuple $\langle \mathcal{S}, \mathcal{A}, \mathcal{P}, \mathcal{R}, \gamma \rangle$:

- $\mathcal{S} = \mathcal{S}_h \times \mathcal{S}_l$ is the continuous state space. $s \in \mathcal{S}$ indicates the state of a user. Considering the session-request structure in sequential recommendation, we decompose \mathcal{S} into two disjoint sub-spaces, i.e., \mathcal{S}_h and \mathcal{S}_l , which is used to represent session-level (high-level) features and request-level (low-level) features, respectively.
- \mathcal{A} is the continuous action space, where $a \in \mathcal{A}$ is a vector representing a recommended item.
- $\mathcal{P} : \mathcal{S} \times \mathcal{A} \times \mathcal{S} \rightarrow \mathbb{R}$ is the transition function, where $p(s_{t+1}|s_t, a_t)$ defines the state transition probability from the current state s_t to the next state s_{t+1} after recommending an item a_t .
- $\mathcal{R} : \mathcal{S} \times \mathcal{A} \rightarrow \mathbb{R}$ is the reward function, where $r(s_t, a_t)$ is the immediate reward by recommending a_t at state s_t . The reward function should be related to return time and/or session length.
- γ is the discount factor for future rewards.

Given a policy $\pi(a|s) : \mathcal{S} \times \mathcal{A} \rightarrow \mathbb{R}$, we define a state-action value function $Q^\pi(s, a)$ which outputs the expected cumulative reward (return) of taking an action a at state s and thereafter following π :

$$Q^\pi(s_t, a_t) = \mathbb{E}_{(s_{t'}, a_{t'}) \sim \pi} \left[r(s_t, a_t) + \sum_{t'=t+1}^{\infty} \gamma^{(t'-t)} \cdot r(s_{t'}, a_{t'}) \right] \quad (1)$$

The optimization objective is to seek a policy $\pi(a|s)$ such that the return obtained by the recommendation agents is maximized:

$$\max_{\pi} \mathcal{J}(\pi) = \mathbb{E}_{s_t \sim d_t^\pi(\cdot), a_t \sim \pi(\cdot|s_t)} [Q^\pi(s_t, a_t)] \quad (2)$$

Here $d_t^\pi(\cdot)$ denotes the state visitation frequency at step t under the policy π .

3 Reinforcing Long-term Engagement with Residual Actor

To improve long-term engagement, we propose to learn a recommendation policy which is broadly consistent to, but better than, the online-serving policy⁵. In this way, i) we have access to sufficient data near the learned policy so that state-action values can be properly estimated because the notorious extrapolation error is minimized [11]; and ii) the potential of harming the user experience is reduced as we can easily control the divergence between the learned new policy and the deployed policy (the online-serving policy) and there is no need to perform online exploration. Despite the advantages, learning such a policy directly is quite difficult because we need to perform optimization in the entire huge policy space. Instead, we solve it by first reconstructing the online-serving policy and then improving it. By doing so, the original optimization problem is decomposed into two sub-tasks which are easier to handle.

Specifically, let $\hat{\pi}(a|s)$ denote the policy we want to learn; we decompose it into $\hat{a} = a_{on} + \Delta(s, a_{on})$ where a_{on} is sampled from the online-serving policy π_{on} , i.e., $a_{on} \sim \pi_{on}(a|s)$, and $\Delta(s, a_{on})$ is the residual which is determined by a deterministic actor. We expect that adding the residual will lead to higher expected return, i.e., $\mathcal{J}(\hat{\pi}) \geq \mathcal{J}(\pi_{on})$. As in Figure 2, our algorithm, ResAct, works in three phases:

- Reconstruction:** ResAct first reconstructs the online-serving policy, i.e., $\tilde{\pi}_{on}(a|s) \approx \pi_{on}(a|s)$, by supervised learning. Then ResAct samples n actions from the reconstructed policy, i.e., $\{\tilde{a}_{on}^i \sim \tilde{\pi}_{on}(a|s)\}_{i=1}^n$ as estimators of a_{on} ;

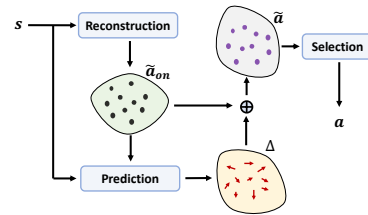


Figure 2: Workflow of ResAct.

⁵The online-serving policy is a historical policy or a mixture of policies which generate logged data to approximate the MDP in sequential recommendation.

- ii) **Prediction:** For each estimator \tilde{a}_{on}^i , ResAct predicts the residual and applies it to \tilde{a}_{on}^i , i.e., $\tilde{a}^i = \tilde{a}_{on}^i + \Delta(s, \tilde{a}_{on}^i)$. We need to learn the residual actor to predict $\Delta(s, \tilde{a}_{on})$ such that \tilde{a} is better than \tilde{a}_{on} in general;
- iii) **Selection:** ResAct selects the best action from the $\{\tilde{a}^i\}_{i=0}^n$ as the final output, i.e., $\arg \max_{\tilde{a}} Q^{\hat{\pi}}(s, \tilde{a})$ for $\tilde{a} \in \{\tilde{a}^i\}_{i=0}^n$.

In sequential recommendation, state representations may not contain sufficient information about long-term engagement. To address this, we design two information-theoretical regularizers to improve the expressiveness and conciseness of the extracted state features. The regularizers are maximizing mutual information between state features and long-term engagement while minimizing the entropy of the state features in order to filter out redundant information. The overview of ResAct is depicted in Figure 3 and we elaborate the details in the subsequent subsections. A formal description for ResAct algorithm is shown in Appendix A.

3.1 Reconstructing Online Behaviors

To reconstruct behaviors of the online-serving policy, we should learn a mapping $\tilde{\pi}_{on}(a|s)$ from states to action distributions such that $\tilde{\pi}_{on}(a|s) \approx \pi_{on}(a|s)$ where $\pi_{on}(a|s)$ is the online-serving policy. A naive approach is to use a model $D(a|s; \theta_d)$ with parameters θ_d to approximate $\pi_{on}(a|s)$ and optimize θ_d by minimizing

$$\mathbb{E}_{s, a_{on} \sim \pi_{on}(a|s)} [(D(a|s; \theta_d) - a_{on})^2] \quad (3)$$

However, such deterministic action generation only allows for an instance of action and will cause huge deviation if the only estimator is not precise. To mitigate this, inspired by conditional variational auto-encoder (CVAE) [16], we propose to encode a_{on} into a latent distribution conditioned on s , and decode samples from the latent space to get estimators of a_{on} . Following CVAE, we define the latent distribution $\mathcal{C}(s, a_{on})$ as a multivariate Gaussian whose parameters, i.e., mean and variance, are determined by an encoder $E(\cdot|s, a_{on}; \theta_e)$ with parameters θ_e . Then for each latent vector $c \sim \mathcal{C}(s, a_{on})$, we can use a decoder $D(a|s, c; \theta_d)$ with parameters θ_d to map it back to an action. To improve generalization ability, we apply a KL regularizer which controls the deviation between $\mathcal{C}(s, a_{on})$ and its prior which is chosen as the multivariate normal distribution $\mathcal{N}(0, 1)$. Formally, we can optimize θ_e and θ_d by minimizing the following loss:

$$L_{\theta_e, \theta_d}^{Rec} = \mathbb{E}_{s, a_{on}, c} [(D(a|s, c; \theta_d) - a_{on})^2 + KL(\mathcal{C}(s, a_{on}; \theta_e) || \mathcal{N}(0, 1))] \quad (4)$$

where $a_{on} \sim \pi_{on}(a|s)$ and $c \sim \mathcal{C}(s, a_{on}; \theta_e)$ ⁶. When performing behavior reconstruction for an unknown state s , we do not know its a_{on} and therefore cannot build $\mathcal{C}(s, a_{on}; \theta_e)$. As a mitigation, we sample n latent vectors from the prior of $\mathcal{C}(s, a_{on})$, i.e., $\{c^i \sim \mathcal{N}(0, 1)\}_{i=0}^n$. Then for each c^i , we can generate an estimator of a_{on} by using the decoder $\tilde{a}_{on}^i = D(a|s, c^i; \theta_d)$.

3.2 Learning to Predict the Optimal Residual

By learning the CVAE which consists of $E(\cdot|s, a_{on}; \theta_e)$ and $D(a|s, c; \theta_d)$, we can easily reconstruct the online-serving policy and sample multiple estimators of a_{on} by $\{\tilde{a}_{on}^i = D(a|s, c^i; \theta_d), c^i \sim \mathcal{N}(0, 1)\}_{i=0}^n$. For each \tilde{a}_{on}^i , we should predict the residual $\Delta(s, \tilde{a}_{on}^i)$ such that $\tilde{a}^i = \tilde{a}_{on}^i + \Delta(s, \tilde{a}_{on}^i)$ is better than \tilde{a}_{on}^i . We use a model $f(\Delta|s, a; \theta_f)$ with parameters θ_f to approximate the residual function $\Delta(s, a)$. Particularly, the residual actor $f(\Delta|s, a; \theta_f)$ consists of a state encoder and a sub-actor, which are for extracting features from a user state and predicting the residual based on the extracted features, respectively. Considering the bi-level session-request structure in sequential recommendation, we design a hierarchical state encoder consisting of a high-level encoder $f_h(s_h; \theta_h)$ and a low-level encoder $f_l(s_l; \theta_l)$ for extracting features from session-level (high-level) state s_h and request-level (low-level) state s_l , respectively. To conclude, the residual actor $f(\Delta|s, a; \theta_f) = \{f_h, f_l, f_a\}$ works as follows:

$$\begin{aligned} z_h &= f_h(s_h; \theta_h); z_l = f_l(s_l; \theta_l) \\ z &= \text{Concat}(z_h, z_l) \\ \Delta &= f_a(z, a; \theta_a) \end{aligned} \quad (5)$$

⁶ $\mathcal{C}(s, a_{on}; \theta_e)$ is parameterized by θ_e because it is a multivariate Gaussian whose mean and variance are the output of the encoder $E(\cdot|s, a_{on}; \theta_e)$.

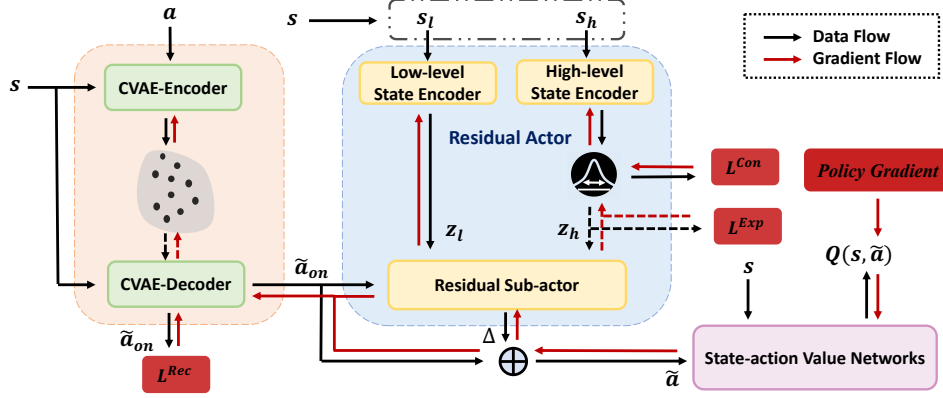


Figure 3: Schematics of our approach. The CVAE-Encoder generates an action embedding distribution, from which a latent vector is sampled for the CVAE-Decoder to reconstruct the action. The reconstructed action \tilde{a}_{on} , together with state features extracted by the high-level and low-level state encoders, are fed to the residual actor to predict the residual Δ . After adding the residual, the action and the state are sent to the state-action value networks, from which policy gradient can be generated. The framework can be trained in an end-to-end manner.

where z_h and z_l are the extracted high-level and low-level features, respectively; z is the concatenation of z_h and z_l , and $f_a(z, a; \theta_a)$ parameterized by θ_a is the sub-actor. Here, $\theta_f = \{\theta_h, \theta_l, \theta_a\}$.

Given a state s and a sampled latent vector $c \sim \mathcal{N}(0, 1)$, ResAct generates an action with a deterministic policy $\hat{\pi}(a|s, c) = D(\tilde{a}_{on}|s, c; \theta_d) + f(\Delta|s, \tilde{a}_{on}; \theta_f)$. We want to optimize the parameters $\{\theta_d, \theta_f\}$ of $\hat{\pi}(a|s, c)$ so that the expected cumulative reward $\mathcal{J}(\hat{\pi})$ is maximized. Based on the Deterministic Policy Gradient (DPG) theorem [26, 20], we derive the following performance gradients (a detailed derivation can be found in Appendix B):

$$\nabla_{\theta_f} \mathcal{J}(\hat{\pi}) = \mathbb{E}_{s,c} [\nabla_a Q^{\hat{\pi}}(s, a)|_{a=\hat{\pi}(a|s,c)} \nabla_{\theta_f} f(\Delta|s, a; \theta_f)|_{a=D(a|s,c;\theta_d)}] \quad (6)$$

$$\nabla_{\theta_d} \mathcal{J}(\hat{\pi}) = \mathbb{E}_{s,c} [\nabla_a Q^{\hat{\pi}}(s, a)|_{a=\hat{\pi}(a|s,c)} \nabla_{\theta_d} D(a|s, c; \theta_d)] \quad (7)$$

Here $\hat{\pi}(a|s, c) = D(\tilde{a}_{on}|s, c; \theta_d) + f(\Delta|s, \tilde{a}_{on}; \theta_f)$, $p(\cdot)$ is the probability function of a random variable, $Q^{\hat{\pi}}(s, a)$ is the state-action value function for $\hat{\pi}$.

To learn the state-action value function, referred to as *critic*, $Q^{\hat{\pi}}(s, a)$ in Eq. (6) and Eq. (7), we adopt Clipped Double Q-learning [10] with two models $Q_1(s, a; \theta_{q_1})$ and $Q_2(s, a; \theta_{q_2})$ to approximate it. For transitions (s_t, a_t, r_t, s_{t+1}) from logged data, we optimize θ_{q_1} and θ_{q_2} to minimize the following Temporal Difference (TD) loss:

$$L_{\theta_{q_j}}^{TD} = \mathbb{E}_{(s_t, a_t, r_t, s_{t+1})} [(Q_j(s_t, a_t; \theta_{q_j}) - y)^2], j = \{1, 2\} \quad (8)$$

$$y = r_t + \gamma \min [Q'_1(s_{t+1}, \hat{\pi}'(a_{t+1}|s_{t+1}); \theta'_{q_1}), Q'_2(s_{t+1}, \hat{\pi}'(a_{t+1}|s_{t+1}); \theta'_{q_2})]$$

where Q'_1, Q'_2 , and $\hat{\pi}'$ are target models whose parameters are soft-updated to match the corresponding models [10].

According to the DPG theorem, we can update the parameters θ_f in the direction of $\nabla_{\theta_f} \mathcal{J}(\hat{\pi})$ to gain a value improvement in $\mathcal{J}(\hat{\pi})$:

$$\theta_f \leftarrow \theta_f + \nabla_{\theta_f} \mathcal{J}(\hat{\pi}), \theta_f = \{\theta_h, \theta_l, \theta_a\} \quad (9)$$

For θ_d , since it also needs to minimize $L_{\theta_d}^{Rec}$, thus the updating direction is

$$\theta_d \leftarrow \theta_d + \nabla_{\theta_d} \mathcal{J}(\hat{\pi}) - \nabla_{\theta_d} L_{\theta_d}^{Rec} \quad (10)$$

Based on $\hat{\pi}(a|s, c)$, theoretically, we can obtain the policy $\hat{\pi}(a|s)$ by marginalizing out the latent vector c : $\hat{\pi}(a|s) = \int p(c) \hat{\pi}(a|s, c) dc$. This integral can be approximated as $\hat{\pi}(a|s) \approx \frac{1}{n} \sum_{i=0}^n \hat{\pi}(a|s, c^i)$ where $\{c^i \sim \mathcal{N}(0, 1)\}_{i=0}^n$. However, given that we already have a critic $Q_1(s, a; \theta_{q_1})$, we can

alternatively use the critic to select the final output:

$$\begin{aligned}\hat{\pi}(a|s) &= \hat{\pi}(a|s, c^*) \\ c^* &= \arg \max_c Q_1(s, \hat{\pi}(a|s, c); \theta_{q1}), c \in \{c^i \sim \mathcal{N}(0, 1)\}_{i=0}^n\end{aligned}\quad (11)$$

3.3 Facilitating Feature Extraction with Information-theoretical Regularizers

Good state representations always ease the learning of models [21]. Considering that session-level states $s_h \in \mathcal{S}_h$ contain rich information about long-term engagement, we design two information-theoretical regularizers to facilitate the feature extraction. Generally, we expect the learned features to have **Expressiveness** and **Conciseness**. To learn features with the desired properties, we propose to encode session-level state s_h into a stochastic embedding space instead of a deterministic vector. Specifically, s_h is encoded into a multivariate Gaussian distribution $\mathcal{N}(\mu_h, \sigma_h)$ whose parameters μ_h and σ_h are predicted by the high-level encoder $f_h(s_h; \theta_h)$. Formally,

$$(\mu_h, \sigma_h) = f_h(s_h; \theta_h), \quad z_h \sim \mathcal{N}(\mu_h, \sigma_h) \quad (12)$$

where z_h is the representation for session-level state s_h . Next, we introduce how to achieve expressiveness and conciseness in z_h .

3.3.1 Expressiveness

We expect the extracted features to contain as much information as possible about long-term engagement rewards, suggesting an intuitive approach to maximize the mutual information between z_h and $r(s, a)$. However, estimating and maximizing mutual information $I_{\theta_h}(z_h; r) = \iint p_{\theta_h}(z_h) p(r|z_h) \log \frac{p(r|z_h)}{p(r)} dz_h dr$ is practically intractable. Instead, we derive a tractable lower bound for the mutual information objective based on variational inference [1]:

$$\begin{aligned}I_{\theta_h}(z_h; r) &\geq \iint p_{\theta_h}(z_h) p(r|z_h) \log \frac{o(r|z_h; \theta_o)}{p(r)} dz_h dr \\ &= \iint p_{\theta_h}(z_h) p(r|z_h) \log o(r|z_h; \theta_o) dz_h dr + H(r)\end{aligned}\quad (13)$$

where $H(r) = -\int p(r) \log p(r) dr$ is the entropy of reward distribution. Since $H(r)$ only depends on user responses and stays fixed for the given environment, we can turn to maximize a lower bound of $I_{\theta_h}(z_h; r)$ which leads to the following expressiveness loss (the derivation is provided in Appendix C):

$$L_{\theta_h, \theta_o}^{Exp} = \mathbb{E}_{s, z_h \sim p_{\theta_h}(z_h|s_h)} [\mathcal{H}(p(r|s) || o(r|z_h; \theta_o))]\quad (14)$$

where s is state, s_h is session-level state, $p_{\theta_h}(z_h|s_h) = \mathcal{N}(\mu_h, \sigma_h)$, and $\mathcal{H}(\cdot || \cdot)$ denotes the cross entropy between two distributions. By minimizing $L_{\theta_h, \theta_o}^{Exp}$, we confirm expressiveness of z_h .

3.3.2 Conciseness

If maximizing $I_{\theta}(z_h; r)$ is the only objective, we could always ensure a maximally informative representation by taking the identity encoding of session-level state ($z_h = s_h$) [1]; however, such an encoding is not useful. Thus, apart from expressiveness, we want z_h to be concise enough to filter out redundant information from s_h . To achieve this goal, we also want to minimize $I_{\theta_h}(z_h; s_h) = \iint p(s_h) p_{\theta_h}(z_h|s_h) \log \frac{p_{\theta_h}(z_h|s_h)}{p_{\theta_h}(z_h)} ds_h dz_h$ such that z_h is the minimal sufficient statistic of s_h for inferring r . Computing the marginal distribution of z_h , $p_{\theta_h}(z_h)$, is usually intractable. So we introduce $m(z_h)$ as a variational approximation to $p_{\theta_h}(z_h)$, which is conventionally chosen as the multivariate normal distribution $\mathcal{N}(0, 1)$. Since $KL(p_{\theta_h}(z_h) || m(z_h)) \geq 0$, we can easily have the following upper bound:

$$I_{\theta_h}(z_h; s_h) \leq \iint p(s_h) p_{\theta_h}(z_h|s_h) \log \frac{p_{\theta_h}(z_h|s_h)}{m(z_h)} ds_h dz_h \quad (15)$$

Minimizing this upper bound leads to the following conciseness loss:

$$\begin{aligned}L_{\theta_h}^{Con} &= \int p(s_h) \left[\int p_{\theta_h}(z_h|s_h) \log \frac{p_{\theta_h}(z_h|s_h)}{m(z_h)} dz_h \right] ds_h \\ &= \mathbb{E}_s [KL(p_{\theta_h}(z_h|s_h) || m(z_h))]\end{aligned}\quad (16)$$

By minimizing $L_{\theta_h}^{Con}$, we achieve conciseness in z_h .

4 Experiment

4.1 Experimental Settings

Dataset. As there is no public dataset that provides information on the length of each session and the time duration between two

sessions, we collected a dataset from a popular streaming platform of short-form videos in Nov. 2021. The dataset contains samples of 99,899 users, including 6,126,583 sessions and 25,921,753 requests. The statistics of the dataset are provided in Table 1, where 25% and 75% denote the corresponding percentile. We didn’t count the average return time, since there are users appearing only once whose return time may go to infinity. We randomly selected 80% of the users as the training set, of which 500 users were reserved for validation. The remaining 20% users constitute the test set. The state of a user contains information about gender, age, and historical interactions such as like rate, forward rate, etc. The item to recommend is determined by comparing the inner product of an action and the embedding of videos [36]. Rewards are designed to measure the **relative** influence of an item on long-term engagement. The details of the reward function are in Appendix D.

Evaluation Metric. We adopt Normalised Capped Importance Sampling (NCIS) [30], a standard offline evaluation method [12, 8], to assess the performance of different policies. Given that π_β is the behavior policy, π is the policy to assess, we evaluate the value by

$$\tilde{J}^{NCIS}(\pi) = \frac{1}{|\mathcal{T}|} \sum_{\xi \in \mathcal{T}} \left[\frac{\sum_{(s,a,r) \in \xi} \tilde{\rho}_{\pi, \pi_\beta}(s, a) r}{\sum_{(s,a,r) \in \xi} \tilde{\rho}_{\pi, \pi_\beta}(s, a)} \right], \quad \tilde{\rho}_{\pi, \pi_\beta}(s, a) = \min \left(c, \frac{\phi_{\pi(s)}(a)}{\phi_{\pi_\beta(s)}(a)} \right) \quad (17)$$

Here \mathcal{T} is the testing set with usage trajectories, $\phi_{\pi(s)}$ denotes a multivariate Gaussian distribution of which mean is given by $\pi(s)$, c is a clipping constant.

Baselines. We compare our method with various baselines, including classic reinforcement learning methods, reinforcement learning with offline training, and imitation learning methods:

- **DDPG** [20]: An reinforcement learning algorithm which concurrently learns a Q-function and a policy. It uses the Q-function to guide the optimization of the policy.
- **TD3** [10]: An off-policy reinforcement learning algorithm which applies clipped double-Q learning, delayed policy updates, and target policy smoothing.
- **TD3_BC** [9]: An reinforcement learning designed for offline training. It adds a behavior cloning (BC) term to the policy update of TD3.
- **BCQ** [11]: An off-policy algorithm which restricts the action space in order to force the agent towards behaving similar to on-policy.
- **IQL** [18]: An offline reinforcement learning method which takes a state conditional upper expextile to estimate the value of the best actions in a state.
- **IL**: Imitation learning treats the training set as expert knowledge and learns a mapping between observations and actions under demonstrations of the expert.
- **IL_CVAE** [16]: Imitation learning method with the policy controlled by a conditional variational auto-encoder.

Our method emphasises on the learning and execution paradigm, and is therefore orthogonal to those approaches which focus on designing neural network architectures, e.g., GRU4Rec [13].

4.2 Overall Performance

To test the performance of ResAct, we conduct experiments with the collected dataset in three modes: i) Return Time mode, where the reward signal is given by $r(\delta)$; ii) Session Length mode, where the reward signal is given by $r(\eta)$; and iii) Both, where reward signal is generated by a convex combination of $r(\delta)$ and $r(\eta)$ with weights of 0.7 and 0.3 respectively. As shown in Table 2, our method significantly outperforms the baselines in all the settings. The classic reinforcement learning algorithms, e.g., DDPG and TD3, perform poorly in the tasks, which indicates that directly predicting an action is difficult. The decomposition of actions effectively facilitates the learning process. Another finding is that the offline reinforcement learning algorithms, e.g., IQL, also perform poorly, even though they are specifically designed to learn from logged data.

Table 1: Statistics of the dataset.

	Users 99,899	Sessions 6,126,583	Requests 25,921,753
	Avg return time (h)	Avg session length	Avg # of sessions
Mean	-	4.0449	61.3277
75%	11.2794	4.8792	85
25%	4.3264	2.1358	30

From the performance comparison with these imitation learning methods, we can infer that the learned residual actor has successfully found a policy to improve an action, because behavior reconstruction alone cannot achieve good performance. To better compare the learning process, we provide learning curves for those RL-based algorithms. Returns are calculated on the validation set of 500 users, with approximately 30,000 sessions. As in Figure 4, the performance of ResAct increases faster and is more stable than the other methods, suggesting that it is easier and more efficient to predict the residual than to predict an action directly.

Table 2: Performance comparison in various tasks. The “ \pm ” indicates 95% confidence intervals.

	Return Time	Session Length	Both
DDPG	0.6375 ± 0.0059	0.3290 ± 0.0056	0.5908 ± 0.0092
TD3	0.6756 ± 0.0133	0.4015 ± 0.0073	0.5498 ± 0.0103
TD3_BC	0.6436 ± 0.0059	0.3671 ± 0.0037	0.5563 ± 0.0050
BCQ	0.6837 ± 0.0061	0.3836 ± 0.0033	0.5915 ± 0.0049
IQL	0.6296 ± 0.0094	0.3430 ± 0.0057	0.5579 ± 0.0067
IL	0.6404 ± 0.0058	0.3186 ± 0.0032	0.5345 ± 0.0048
IL_CVAE	0.6410 ± 0.0058	0.3178 ± 0.0031	0.5346 ± 0.0047
ResAct (Ours)	0.7980 ± 0.0067	0.5433 ± 0.0045	0.6675 ± 0.0053

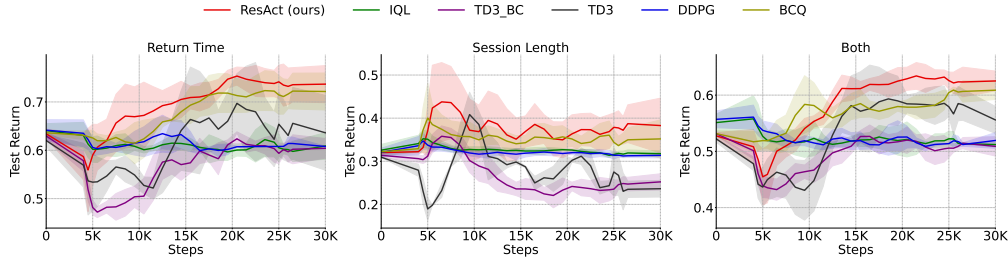


Figure 4: Learning curves of RL-based methods. Returns are calculated on the validation set.

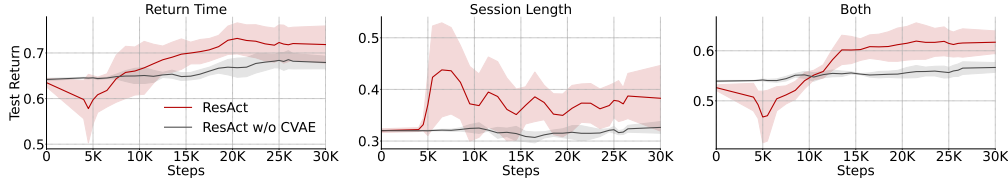


Figure 5: Learning curves for ResAct with CVAE and a deterministic reconstructor (w/o CVAE).

4.3 Analyses and Ablations

How does ResAct work? To understand the working process of ResAct, we plot t-SNE [33] embedding of actions generated in the execution phase of ResAct. As in Figure 6, the reconstructed actions, denoted by the red dots, are located around the initial action (the red star), suggesting that ResAct successfully samples several online-behavior estimators. The blue dots are the t-SNE embedding of the improved actions, which are generated by imposing residuals on the reconstructed actions. The blue star denotes the executed action of ResAct. We can find that the blue dots are near the initial actions but cover a wider area than the red dots.

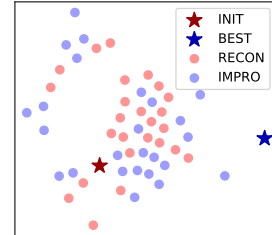


Figure 6: The t-SNE visualization of actions.

Effect of the CVAE. We design the CVAE for online-behavior reconstruction because of its ability to generate multiple estimators. To explore the effect of the CVAE and whether a deterministic action reconstructor can achieve similar performance, we disable the CVAE in ResAct and replace it with a feed-forward neural network. The feed-forward neural network is trained by using the loss in Equation 3. Since the feed-forward neural network is deterministic, ResAct does not need to perform the selection phase as there is only one candidate action. We provide the learning curves of ResAct with and without the CVAE in Figure 5. As we can find, there is no significant improvement in performance if we disable the CVAE. We deduce that this is because a deterministic behavior reconstructor can only generate one estimator, and if the prediction is inaccurate, performance will be severely harmed.

Number of Online-behavior Estimators. Knowing that generating only one action estimator might hurt performance, we want to further investigate how the number of estimators will affect the performance of ResAct. We first train a ResAct and then change the number of

online-behavior estimators to 5, 10, 15, 20 and 25. As in Figure 7, consistent improvement in performance can be observed across all the three tasks as we increase the number of estimators. The fact suggests that generating more action candidates will benefit the performance, in line with our intuition. Because the sampling of action estimators is independent, the parallelization of ResAct is not difficult to implement and we can easily speed up the inference of ResAct.

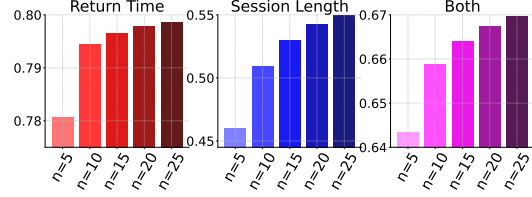


Figure 7: Ablations for the number of online-behavior estimators.

Information-theoretical Regularizers. To explore the effect of the designed regularizers, we disable $L_{\theta_h, \theta_o}^{Exp}$, $L_{\theta_h}^{Con}$ and both of them in ResAct, respectively. As shown in Table 3, the removal of any of the regularizers results in a significant drop in performance, suggesting that the regularizers facilitate the extraction of features and thus ease the learning process. An interesting finding is that removing both of the regularizers does not necessarily results in worse performance than removing only one (e.g., in the Return Time task). This suggests that we cannot simply expect either expressiveness or conciseness of features separately, but rather combination of both expressiveness and conciseness. These two regularizers work together to learn better state representations.

Table 3: Ablations for the information-theoretical regularizers. The “ \pm ” indicates 95% confidence intervals.

	Return Time	Session Length	Both
ResAct	0.7980 \pm 0.0067	0.5433 \pm 0.0045	0.6675 \pm 0.0053
w/o $L_{\theta_h, \theta_o}^{Exp}$	0.6610 \pm 0.0060	0.3895 \pm 0.0034	0.6074 \pm 0.0052
w/o $L_{\theta_h}^{Con}$	0.6944 \pm 0.0061	0.4542 \pm 0.0038	0.6041 \pm 0.0051
w/o $L_{\theta_h, \theta_o}^{Exp}, L_{\theta_h}^{Con}$	0.7368 \pm 0.0064	0.3854 \pm 0.0033	0.6348 \pm 0.0049

5 Related Work

Sequential Recommendation. Sequential recommendation has been used to model real-world recommendation problems where the browse length is not fixed [39]. Many existing works focused on encoding user previous records with various neural network architectures. For example, GRU4Rec [13] utilizes Gated Recurrent Unit to exploit users’ interaction histories; BERT4Rec [28] employs a deep bidirectional self-attention structure to learn sequential patterns. However, these works focus on optimizing immediate engagement like click-through rates. FeedRec [41] was proposed to improve long-term engagement in sequential recommendation. However, it is based on strong assumption that recommendation diversity will lead to improvement in user stickiness.

Reinforcement Learning in Recommender Systems. Reinforcement learning (RL) has attracted much attention from the recommender system research community for its ability to capture potential future rewards [40, 37, 41, 38, 3]. Shani et al. [25] first proposed to treat recommendation as a Markov Decision Process (MDP), and designed a model-based RL method for book recommendation. Dulac-Arnold et al. [7] brought RL to MDPs with large discrete action spaces and demonstrated the effectiveness on various recommendation tasks with up to one million actions. Chen et al. [2] scaled a batch RL algorithm, i.e., REINFORCE with off-policy correction to real-world products serving billions of users. Despite the success, previous work required RL agents to learn in the entire policy space. Considering the expensive online interactions and huge state-action spaces, learning the optimal policy in the entire MDP is quite difficult. Our method instead learns a policy near the online-serving policy, which is much easier.

6 Conclusion

In this work, we propose ResAct to reinforce long-term engagement in sequential recommendation. ResAct works by first reconstructing behaviors of the online-serving policy, and then improving the reconstructed policy by imposing a residual which is predicted by the residual actor. By doing so, ResAct learns a policy which is close to, but better than, the deployed recommendation model. To facilitate the feature extraction, two information-theoretical regularizers are designed to make state representations both expressive and concise. We conduct extensive experiments with a real-world dataset. The experimental results show that our method significantly outperforms the state-of-the-art algorithms in various long-term engagement optimization tasks.

References

- [1] A. A. Alemi, I. Fischer, J. V. Dillon, and K. Murphy. Deep variational information bottleneck. *ICLR*, 2017.
- [2] M. Chen, A. Beutel, P. Covington, S. Jain, F. Belletti, and E. H. Chi. Top-k off-policy correction for a reinforce recommender system. In *Proceedings of the 12th ACM International Conference on Web Search and Data Mining*, pages 456–464, 2019.
- [3] M. Chen, Y. Wang, C. Xu, Y. Le, M. Sharma, L. Richardson, S.-L. Wu, and E. Chi. Values of user exploration in recommender systems. In *Proceedings of the 15th ACM Conference on Recommender Systems*, pages 85–95, 2021.
- [4] X. Chen, H. Xu, Y. Zhang, J. Tang, Y. Cao, Z. Qin, and H. Zha. Sequential recommendation with user memory networks. In *Proceedings of the 11th ACM International Conference on Web Search and Data Mining*, pages 108–116, 2018.
- [5] G. de Souza Pereira Moreira, S. Rabhi, J. M. Lee, R. Ak, and E. Oldridge. Transformers4rec: Bridging the gap between nlp and sequential/session-based recommendation. In *Proceedings of the 15th ACM Conference on Recommender Systems*, pages 143–153, 2021.
- [6] T. Donkers, B. Loepp, and J. Ziegler. Sequential user-based recurrent neural network recommendations. In *Proceedings of the 11th ACM Conference on Recommender Systems*, pages 152–160, 2017.
- [7] G. Dulac-Arnold, R. Evans, H. van Hasselt, P. Sunehag, T. Lillicrap, J. Hunt, T. Mann, T. Weber, T. Degris, and B. Coppin. Deep reinforcement learning in large discrete action spaces. *arXiv preprint arXiv:1512.07679*, 2015.
- [8] M. Farajtabar, Y. Chow, and M. Ghavamzadeh. More robust doubly robust off-policy evaluation. In *ICML*, pages 1447–1456, 2018.
- [9] S. Fujimoto and S. S. Gu. A minimalist approach to offline reinforcement learning. *NeurIPS*, 34, 2021.
- [10] S. Fujimoto, H. Hoof, and D. Meger. Addressing function approximation error in actor-critic methods. In *ICML*, pages 1587–1596, 2018.
- [11] S. Fujimoto, D. Meger, and D. Precup. Off-policy deep reinforcement learning without exploration. In *ICML*, pages 2052–2062, 2019.
- [12] A. Gilotte, C. Calauzènes, T. Nedelec, A. Abraham, and S. Dollé. Offline a/b testing for recommender systems. In *Proceedings of the 11th ACM International Conference on Web Search and Data Mining*, pages 198–206, 2018.
- [13] B. Hidasi, A. Karatzoglou, L. Baltrunas, and D. Tikk. Session-based recommendations with recurrent neural networks. In *ICLR*, 2016.
- [14] J. Huang, W. X. Zhao, H. Dou, J.-R. Wen, and E. Y. Chang. Improving sequential recommendation with knowledge-enhanced memory networks. In *The 41st International ACM SIGIR Conference on Research & Development in Information Retrieval*, pages 505–514, 2018.
- [15] D. P. Kingma and J. Ba. Adam: A method for stochastic optimization. *arXiv preprint arXiv:1412.6980*, 2014.
- [16] D. P. Kingma and M. Welling. Auto-encoding variational bayes. In *ICML*, 2014.
- [17] B. R. Kiran, I. Sobh, V. Talpaert, P. Mannion, A. A. Al Sallab, S. Yogamani, and P. Pérez. Deep reinforcement learning for autonomous driving: A survey. *IEEE Transactions on Intelligent Transportation Systems*, 2021.
- [18] I. Kostrikov, A. Nair, and S. Levine. Offline reinforcement learning with in-sample q-learning. In *ICLR*, 2022.
- [19] S. Levine, C. Finn, T. Darrell, and P. Abbeel. End-to-end training of deep visuomotor policies. *The Journal of Machine Learning Research*, 17(1):1334–1373, 2016.
- [20] T. P. Lillicrap, J. J. Hunt, A. Pritzel, N. Heess, T. Erez, Y. Tassa, D. Silver, and D. Wierstra. Continuous control with deep reinforcement learning. *ICLR*, 2016.
- [21] M. A. Nielsen. *Neural networks and deep learning*, volume 25. Determination press San Francisco, CA, USA, 2015.

- [22] B. L. Pereira, A. Ueda, G. Penha, R. L. Santos, and N. Ziviani. Online learning to rank for sequential music recommendation. In *Proceedings of the 13th ACM Conference on Recommender Systems*, pages 237–245, 2019.
- [23] J. Rappaz, J. McAuley, and K. Aberer. *Recommendation on live-streaming platforms: dynamic availability and repeat consumption*, page 390–399. 2021.
- [24] J. Schrittwieser, I. Antonoglou, T. Hubert, K. Simonyan, L. Sifre, S. Schmitt, A. Guez, E. Lockhart, D. Hassabis, T. Graepel, et al. Mastering atari, go, chess and shogi by planning with a learned model. *Nature*, 588(7839):604–609, 2020.
- [25] G. Shani, D. Heckerman, R. I. Brafman, and C. Boutilier. An mdp-based recommender system. *JMLR*, 6(9), 2005.
- [26] D. Silver, G. Lever, N. Heess, T. Degris, D. Wierstra, and M. Riedmiller. Deterministic policy gradient algorithms. In *ICML*, pages 387–395, 2014.
- [27] D. Silver, J. Schrittwieser, K. Simonyan, I. Antonoglou, A. Huang, A. Guez, T. Hubert, L. Baker, M. Lai, A. Bolton, et al. Mastering the game of go without human knowledge. *Nature*, 550(7676):354–359, 2017.
- [28] F. Sun, J. Liu, J. Wu, C. Pei, X. Lin, W. Ou, and P. Jiang. Bert4rec: Sequential recommendation with bidirectional encoder representations from transformer. In *Proceedings of the 28th ACM International Conference on Information and Knowledge Management*, pages 1441–1450, 2019.
- [29] R. S. Sutton and A. G. Barto. *Reinforcement learning: An introduction*. MIT press, 2018.
- [30] A. Swaminathan and T. Joachims. The self-normalized estimator for counterfactual learning. *NeurIPS*, 28, 2015.
- [31] J. Tang and K. Wang. Personalized top-n sequential recommendation via convolutional sequence embedding. In *Proceedings of the 11th ACM International Conference on Web Search and Data Mining*, pages 565–573, 2018.
- [32] C. H. Teo, H. Nassif, D. Hill, S. Srinivasan, M. Goodman, V. Mohan, and S. Vishwanathan. Adaptive, personalized diversity for visual discovery. In *Proceedings of the 10th ACM Conference on Recommender Systems*, pages 35–38, 2016.
- [33] L. Van der Maaten and G. Hinton. Visualizing data using t-sne. *Journal of machine learning research*, 9(11), 2008.
- [34] S. Wang, L. Hu, Y. Wang, L. Cao, Q. Z. Sheng, and M. Orgun. Sequential recommender systems: Challenges, progress and prospects. In *IJCAI*, pages 6332–6338, 2019.
- [35] Q. Wu, H. Wang, L. Hong, and Y. Shi. Returning is believing: Optimizing long-term user engagement in recommender systems. In *Proceedings of the 2017 ACM on Conference on Information and Knowledge Management*, pages 1927–1936, 2017.
- [36] D. Zhao, L. Zhang, B. Zhang, L. Zheng, Y. Bao, and W. Yan. Mahrl: Multi-goals abstraction based deep hierarchical reinforcement learning for recommendations. In *Proceedings of the 43rd International ACM SIGIR Conference on Research and Development in Information Retrieval*, pages 871–880, 2020.
- [37] X. Zhao, L. Zhang, Z. Ding, L. Xia, J. Tang, and D. Yin. Recommendations with negative feedback via pairwise deep reinforcement learning. In *Proceedings of the 24th ACM SIGKDD International Conference on Knowledge Discovery & Data Mining*, pages 1040–1048, 2018.
- [38] X. Zhao, X. Zheng, X. Yang, X. Liu, and J. Tang. Jointly learning to recommend and advertise. In *Proceedings of the 26th ACM SIGKDD International Conference on Knowledge Discovery & Data Mining*, pages 3319–3327, 2020.
- [39] Y. Zhao, Y.-H. Zhou, M. Ou, H. Xu, and N. Li. Maximizing cumulative user engagement in sequential recommendation: An online optimization perspective. In *Proceedings of the 26th ACM SIGKDD International Conference on Knowledge Discovery & Data Mining*, pages 2784–2792, 2020.
- [40] G. Zheng, F. Zhang, Z. Zheng, Y. Xiang, N. J. Yuan, X. Xie, and Z. Li. Drn: A deep reinforcement learning framework for news recommendation. In *WWW*, pages 167–176, 2018.
- [41] L. Zou, L. Xia, Z. Ding, J. Song, W. Liu, and D. Yin. Reinforcement learning to optimize long-term user engagement in recommender systems. In *Proceedings of the 25th ACM SIGKDD International Conference on Knowledge Discovery & Data Mining*, pages 2810–2818, 2019.

A Overall Algorithm

We provide the learning process of ResAct in Algorithm 1. Particularly, the CVAE is trained to reconstruct the online-serving policy, the residual actor is trained for predicting the optimal residual for each reconstructed action, and the critic networks is trained to guide the optimization of the decoder in CVAE and the residual actor. For the target networks (line 2), $\{\theta_d, \theta_h, \theta_l, \theta_a, \theta_{q_1}\}$ is for the target policy, and $\{\theta_{q_1}, \theta_{q_2}\}$ is for the target critics. The execution process of ResAct is summarized in Algorithm 2. Only the decoder of the CVAE, the residual actor and one of the critics are used during execution.

Algorithm 1: ResAct-LEARNING

Input: Logged data collected by the online-serving policy $\mathcal{D} = \{(s_t, a_t, r_t, s_{t+1})\}$

- 1 Initialize the CVAE: $\{E(c|s, a; \theta_e), D(a|s, c; \theta_d)\}$, the residual actor: $\{f_h(z_h|s_h; \theta_h), f_l(z_l|s_l; \theta_l), f_a(\Delta|z, a; \theta_a)\}$, the critic networks $\{Q_1(s, a; \theta_{q_1}), Q_2(s, a; \theta_{q_2})\}$, and the variational estimator $o(r|z_h; \theta_o)$
- 2 Set soft-update rate τ and initialize the target networks $\theta' \leftarrow \theta$ for $\theta \in \{\theta_d, \theta_h, \theta_l, \theta_a, \theta_{q_1}, \theta_{q_2}\}$
- 3 **for** $k = 1$ **to** K **do**
- 4 Sample a batch of transitions (s_t, a_t, r_t, s_{t+1}) from \mathcal{D}
- 5 $\theta_e \leftarrow \theta_e - \nabla_{\theta_e} L_{\theta_e, \theta_d}^{Rec}$ ($L_{\theta_e, \theta_d}^{Rec}$ is in Eq. 4)
- 6 Update θ_d according to Eq. 10
- 7 Update $\{\theta_h, \theta_l, \theta_a\}$ according to Eq. 9
- 8 $\theta_{q_j} \leftarrow \theta_{q_j} - \nabla_{\theta_{q_j}} L_{\theta_{q_j}}^{TD}, j = \{1, 2\}$ ($L_{\theta_{q_j}}^{TD}$ is in Eq. 8)
- 9 $\theta_h \leftarrow \theta_h - \nabla_{\theta_h} L_{\theta_h, \theta_o}^{Exp} - \nabla_{\theta_h} L_{\theta_h}^{Con}$
- 10 $\theta_o \leftarrow \theta_o - \nabla_{\theta_o} L_{\theta_h, \theta_o}^{Exp}$
- 11 ($L_{\theta_h, \theta_o}^{Exp}$ is in Eq. 14, and $L_{\theta_h}^{Con}$ is in Eq. 16)
- 11 Update the target networks:
 $\theta' \leftarrow \tau\theta + (1 - \tau)\theta'$ for $\theta \in \{\theta_d, \theta_h, \theta_l, \theta_a, \theta_{q_1}, \theta_{q_2}\}$
- 12 **end**

Algorithm 2: ResAct-EXECUTION

Input: State s , number of estimators n

// Reconstruction

- 1 Generate n estimators of a_{on} : $\{\tilde{a}_{on}^i = D(a|s, c^i; \theta_d), c^i \sim \mathcal{N}(0, 1)\}_{i=0}^n$

// Prediction

- 2 **for** $\tilde{a}_{on} \in \{\tilde{a}_{on}^i\}_{i=0}^n$ **do**
- 3 Predict the residual $\Delta = f(\Delta|s, \tilde{a}_{on}; \theta_f)$ as in Eq. 5
- 4 Apply the residual: $\tilde{a} = \tilde{a}_{on} + \Delta$
- 5 **end**

// Selection

- 6 $a^* = \arg \max_a Q_1(s, a; \theta_{q_1}), a \in \{\tilde{a}^i\}_{i=0}^n$

Output: Action a^*

B The Derivation of Performance Gradients

We begin by deriving the gradients of $\mathcal{J}(\hat{\pi})$ with respect to the parameters of the residual actor.

$$\begin{aligned}\nabla_{\theta_f} \mathcal{J}(\hat{\pi}) &= \iint p(c)p^{\hat{\pi}}(s) \nabla_a Q^{\hat{\pi}}(s, a)|_{a=\hat{\pi}(a|s, c)} \nabla_{\theta_f} \hat{\pi}(a|s, c) dc ds \\ &= \iint p(c)p^{\hat{\pi}}(s) \nabla_a Q^{\hat{\pi}}(s, a)|_{a=\hat{\pi}(a|s, c)} \nabla_{\theta_f} f(\Delta|s, a; \theta_f)|_{a=D(a|s, c; \theta_d)} dc ds \\ &= \mathbb{E}_{s, c} [\nabla_a Q^{\hat{\pi}}(s, a)|_{a=\hat{\pi}(a|s, c)} \nabla_{\theta_f} f(\Delta|s, a; \theta_f)|_{a=D(a|s, c; \theta_d)}]\end{aligned}\quad (18)$$

The decoder $D(a|s, c; \theta_d)$ also affects the policy. The gradients of $\mathcal{J}(\hat{\pi})$ with respect to θ_d is derived similarly:

$$\begin{aligned}\nabla_{\theta_d} \mathcal{J}(\hat{\pi}) &= \iint p(c)p^{\hat{\pi}}(s) \nabla_a Q^{\hat{\pi}}(s, a)|_{a=\hat{\pi}(a|s, c)} \nabla_{\theta_d} \hat{\pi}(a|s, c) dc ds \\ &= \iint p(c)p^{\hat{\pi}}(s) \nabla_a Q^{\hat{\pi}}(s, a)|_{a=\hat{\pi}(a|s, c)} \nabla_{\theta_d} D(a|s, c; \theta_d) dc ds \\ &= \mathbb{E}_{s, c} [\nabla_a Q^{\hat{\pi}}(s, a)|_{a=\hat{\pi}(a|s, c)} \nabla_{\theta_d} D(a|s, c; \theta_d)]\end{aligned}\quad (19)$$

C Deriving the Expressiveness Loss

We expect the extracted features to contain as much information as possible about long-term engagement rewards, suggesting an intuitive approach to maximize the mutual information between z_h and $r(s, a)$. The mutual information $I_{\theta_h}(z_h; r)$ is defined according to

$$\begin{aligned}I_{\theta_h}(z_h; r) &= \iint p(z_h, r) \log \frac{p(z_h, r)}{p(z_h)p(r)} dz_h dr \\ &= \iint p_{\theta_h}(z_h)p(r|z_h) \log \frac{p(r|z_h)}{p(r)} dz_h dr\end{aligned}\quad (20)$$

However, estimating and maximizing mutual information is practically intractable. Inspired by variational inference [1], we derive a tractable lower bound for the mutual information objective. Considering that $KL(p(r|z_h)||q(r|z_h)) \geq 0$, by the definition of KL-divergence, we have $\int p(r|z_h) \log p(r|z_h) dr \geq \int p(r|z_h) \log q(r|z_h) dr$ where $q(r|z_h)$ is an arbitrary distribution. Here, we introduce $o(r|z_h; \theta_o)$ as a variational neural estimator with parameters θ_o of $p(r|z_h)$. Then,

$$\begin{aligned}I_{\theta_h}(z_h; r) &\geq \iint p_{\theta_h}(z_h)p(r|z_h) \log \frac{o(r|z_h; \theta_o)}{p(r)} dz_h dr \\ &= \iint p_{\theta_h}(z_h)p(r|z_h) \log o(r|z_h; \theta_o) dz_h dr + H(r)\end{aligned}\quad (21)$$

where $H(r) = -\int p(r) \log p(r) dr$ is the entropy of reward distribution. Since $H(r)$ only depends on user responses and stays fixed for the given environment, we can turn to maximize a lower bound of $I_{\theta_h}(z_h; r)$ which leads to the following expressiveness loss:

$$\begin{aligned}L_{\theta_h, \theta_o}^{Exp} &= - \iint p_{\theta_h}(z_h)p(r|z_h) \log o(r|z_h; \theta_o) dz_h dr \\ &= - \iiint p(s)p_{\theta_h}(z_h|s)p(r|s, z_h) \log o(r|z_h; \theta_o) ds dz_h dr \\ &= - \iiint p(s)p_{\theta_h}(z_h|s_h)p(r|s) \log o(r|z_h; \theta_o) ds dz_h dr \\ &= \mathbb{E}_{s, z_h \sim p_{\theta_h}(z_h|s_h)} \left[- \int p(r|s) \log o(r|z_h; \theta_o) dr \right] \\ &= \mathbb{E}_{s, z_h \sim p_{\theta_h}(z_h|s_h)} [\mathcal{H}(p(r|s)||o(r|z_h; \theta_o))]\end{aligned}\quad (22)$$

where s is state, s_h is session-level state, $p_{\theta_h}(z_h|s_h) = \mathcal{N}(\mu_h, \sigma_h)$, and $\mathcal{H}(\cdot||\cdot)$ denotes the cross entropy between two distributions. By minimizing $L_{\theta_h, \theta_o}^{Exp}$, we confirm expressiveness of z_h .

D Designing the Reward Function

The rewards of long-term engagement are designed based on the statistics of the dataset. As a general guideline, we expect rewards to reflect the influence of recommending an item on a user. However, behaviors of users have large variance which makes the influence difficult to measure. For example, if we simply make rewards proportional to session length, or inversely proportional to return time, the recommender system would focus on improving the experience of high activity users, because by doing so it can obtain larger rewards. However, in reality, it is equally if not more important to facilitate the conversion of low activity user to high activity user, which requires us to improve the experience of low activity users. To address this issue, we turn to measuring the **relative** influence of an item. Concretely, we calculate the average return time δ_{avg}^u and the average session length η_{avg}^u for a user u , and use these two statistics to quantify rewards. For user u , given a time duration δ^u between two sessions, the corresponding reward is calculated by

$$r(\delta^u) = \left(\lfloor \frac{\min(\delta_{avg}^u, \delta_{75\%})}{\delta^u} \rfloor \right) .clip(0, 5) \quad (23)$$

where $\delta_{75\%}$ is the 75th percentile of the average return time for all users, which is designed to differentiate active users and inactive users. Rewards for the session length is calculated similarly as

$$r(\eta^u) = \left(\lfloor \frac{\eta^u}{\eta_{avg}^u \times 0.8} \rfloor \right) .clip(0, 5) \quad (24)$$

where η^u is the length of a session in the logged data of user u . Since δ^u and δ can only be calculated at session-level, without loss of generality, we provide rewards at the end of each session, where rewards for return time is assigned to the previous session.

E Experimental Details

Across all methods and experiments, for fair comparison, each network generally uses the same architecture (3-layers MLP with 256 neurons at each hidden layer) and hyper-parameters. We provide the hyper-parameters for ResAct in Table 4. All methods are implemented with PyTorch.

Table 4: Hyper-parameters of ResAct.

Hyper-parameter	Value
Optimizer	Adam [15]
Actor Learning Rate	5×10^{-6}
Critic Learning Rate	5×10^{-5}
Batch Size	4096
Normalized Observations	Ture
Gradient Clipping	False
Discount Factor	0.9
Number of Behavior Estimators	20
Weight of L^{Exp}	5×10^{-2}
Weight of L^{Con}	5×10^{-1}
Target Update Rate	1×10^{-2}
Number of Epoch	5

F Additional Experimental Results

Apart from the large-scale real-world dataset, we also conduct experiments on some representative benchmark dataset. MovieLens-1m is a popular benchmark dataset for evaluating recommendation algorithms. It provides 1,000,209 anonymous ratings of approximately 3,900 movies made by 6,040 MovieLens users. Ratings are made on a 5-star scale. We sample the data of 5000 users as the training set, and use the data of the remaining users as the test set (with 50 users as the validation set). As MovieLens-1m does not contain any information about long-term user engagement, we make an assumption that the user engagement is proportional to the movie ratings. Specifically, we assume that recommending a movie for which a user rates 2-stars will not affect engagement, a movie with 3-stars, 4-stars and 5-stars will benefit the long-term engagement by 1, 2, and 3, respectively. Recommending a movie with 1-star is harmful to engagement and will be given a negative reward, -1. The objective of recommendation is to maximize the cumulative ratings so that long-term engagement could be improved. We use NCIS to assess the performance. As in Table 5, our method, ResAct, outperforms all the baselines, indicating its effectiveness. We also provide the learning curve in Figure 8. It can be found that ResAct learns faster and more stable than the baselines.

Table 5: Performance comparison in MovieLens-1m. The “ \pm ” indicates 95% confidence intervals.

	Return
DDPG	1.7429 ± 0.0545
TD3	1.7363 ± 0.0546
TD3_BC	1.7135 ± 0.0541
BCQ	1.7898 ± 0.0320
IQL	1.7360 ± 0.0546
IL	1.7485 ± 0.0310
IL_CVAE	1.7344 ± 0.0316
ResAct (Ours)	1.8123 ± 0.0319

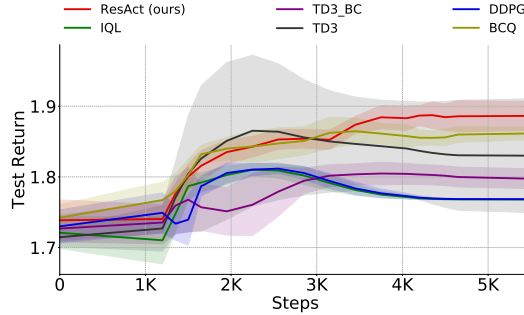


Figure 8: Learning curves of RL-based methods on MovieLens-1m. Returns are calculated on the validation set.